Measurements of heavy flavours with the ALICE experiment at LHC

Denise Moreira de Godoy[*] **on behalf of the ALICE Collaboration** [†]

Institut für Kernphysik
Westfälische Wilhelms-Universität Münster
Wilhelm-Klemm-Str. 9 - 48149 Münster - Germany
E-mail: moreirad@uni-muenster.de

The ALICE collaboration has measured the production of open heavy flavours via their hadronic and semi-electronic decays at mid-rapidity and via their semi-muonic decay channel at forward rapidity in pp collisions at $\sqrt{s}$ = 2.76 and 7 TeV, p–Pb collisions at $\sqrt{s_{NN}}$ = 5.02 TeV, and Pb–Pb collisions at $\sqrt{s_{NN}}$ = 2.76 TeV. We present the ALICE results on the nuclear modification factor, elliptic flow, and azimuthal angular correlations of open heavy-flavour hadrons. The results are compared with model calculations.

54th International Winter Meeting on Nuclear Physics
25-29 January 2016
Bormio, Italy

---

[*]Speaker.
[†]This work was supported by BMBF (FSP201-ALICE).

1. Introduction

The main goal of the ALICE experiment is to study the state of matter created in ultra-relativistic heavy-ion collisions at the LHC. According to Quantum Chromodynamics (QCD) calculations on the lattice, the energy density and temperature reached in these collisions are sufficiently high for a phase transition of the nuclear matter to a deconfined state of quarks and gluons [1, 2]. Heavy quarks, i.e. charm and beauty, are mainly produced in hard parton scattering processes at the initial stage of the collisions, because of their large masses. Therefore, they experience the complete evolution of the system created in heavy-ion collisions at high energies, losing energy via radiative and collisional scattering processes in the interaction with the medium constituents. According to QCD calculations, the energy loss of the partons traversing the medium depends on the colour charge and the mass of the parton, leading to a hierarchy where beauty quarks lose less energy than charm quarks, and charm quarks lose less energy than light quarks and gluons [3, 4, 5].

The in-medium energy loss of heavy quarks can be investigated with the nuclear modification factor (R_{AA}) of heavy-flavour hadrons and their decay products, which is defined by the ratio of the yield of particles in heavy-ion collisions with respect to the binary scaled yield in pp collisions. By construction, R_{AA} is expected to be unity in absence of nuclear effects. The energy loss of heavy flavours in the medium causes a suppression of heavy-flavour particle yields, R_{AA} < 1, at intermediate-high transverse momentum (p_T). The nuclear modification factor is measured in proton-nucleus collisions in order to study the cold nuclear matter (CNM) effects on the heavy-flavour production in heavy-ion collisions as, for instance, nuclear modification of the parton distribution functions [6, 7] and possible saturation of the low-x gluon density [8].

The created matter can be studied complementarily with the azimuthal anisotropy of heavy-flavour hadrons and their decay products in momentum space. The particle azimuthal distribution in momentum space can be expressed as a Fourier series with respect to the reaction plane (RP), which is defined by the impact parameter direction of the colliding nuclei and the beam direction. In heavy-ion collisions, the second harmonic of the distribution v_2, called elliptic flow, quantifies the elliptic azimuthal anisotropy of the emitted particles. The elliptic flow of heavy-flavour particles at low p_T is sensitive to the collective motion of heavy quarks in the medium caused by pressure gradients. Because of the almond-shaped overlap area in non-central heavy-ion collisions, particles emitted along the minor axis of the ellipsoid (in-plane direction) traverse less medium on average with respect to particles emitted along the major axis of the ellipsoid (out-of-plane direction). Therefore, the measurement of the v_2 coefficient of heavy-flavour particles at high p_T can constrain the path-length dependence of the energy loss of heavy quarks.

Further investigation of the medium created in heavy-ion collisions can be provided with the two-particle azimuthal angular correlations involving heavy-flavour particles. The azimuthal angular correlation distributions in heavy-ion collisions is sensitive to the nuclear modification of heavy quark fragmentation functions. The measurement in proton-nucleus collisions can be used to investigate CNM effects and the potential existence of collective phenomena in such collisions [9]. In addition, the azimuthal angular correlations between electrons from heavy-flavour decays and charged particles in pp collisions can be used to estimate the relative contribution of electrons from beauty-hadron decays to the yield of electrons from heavy-flavour decays.

2. ALICE experiment and particle identification

The ALICE detector consists of various detectors for particle reconstruction, triggering and event characterization. In the following, only the ALICE subsystems that are relevant for the presented open heavy-flavour analyses are described. More details of the ALICE detector can be found in [10, 11].

Charged particles are reconstructed and identified with the Inner Tracking System (ITS), the Time Projection Chamber (TPC), the Time-Of-Flight (TOF) detectors at mid-rapidity ($|\eta| < 0.9$). Electrons are also identified with the ElectroMagnetic Calorimeter (EMCal) at mid-rapidity ($|\eta| < 0.7$). Muons are reconstructed and identified with the Muon Spectrometer at forward rapidity ($-4 < \eta < -2.5$). The V0 detector, which consists of the scintillator counters V0A at backward rapidity ($2.8 < \eta < 5.1$) and V0C at forward rapidity ($-3.7 < \eta < -1.7$), and the Zero Degree Calorimeters (ZDC) are used for triggering and event selection. The V0 detector is also used to estimate the reaction plane direction of the event.

The production of open heavy flavours has been measured with ALICE via their hadronic and semi-electronic decays at mid-rapidity and via their semi-muonic decay channel at forward rapidity in pp collisions at $\sqrt{s}$ = 2.76 and 7 TeV, p–Pb collisions at $\sqrt{s_{NN}}$ = 5.02 TeV, and Pb–Pb collisions at $\sqrt{s_{NN}}$ = 2.76 TeV.

Charm mesons are reconstructed via the following hadronic decay channels: $D^0 \to K^- \pi^+$, $D^+ \to K^- \pi^+ \pi^+$, $D^{\star+} \to D^0(\to K^- \pi^+)\pi^+$, $D_s^+ \to \phi(\to K^- K^+)\pi^+$, and their charge conjugates. D-meson decay particles are reconstructed and identified with the ITS, TPC and TOF detectors. The decay topologies are reconstructed based on the displacement of the decay particles with respect to the primary vertex, for instance, the separation between the primary and secondary vertices and the pointing angle of the reconstructed D-meson momentum [12]. The D-meson yields are extracted from fits to the invariant mass distributions for D^0, D^+ and D_s^+ candidates and from mass difference $\Delta M = M(K\pi\pi) - M(K\pi)$ distributions for $D^{\star+}$ candidates. The contribution of the secondary D mesons from B-meson decays is estimated using perturbative QCD (pQCD) calculations of the B-meson production [13] and Monte Carlo (MC) simulations.

The electron candidates are reconstructed with the ITS, TPC, TOF and EMCal detectors. The electron sample is composed of electrons from heavy-flavour hadron decays and from background sources, which are mainly electrons from photon conversions in detector material and from Dalitz decays of neutral mesons. The contribution of electrons that do not originate from heavy-flavour hadron decays is obtained using the invariant mass of electron-positron pairs, which is expected to have small values for pairs coming from photon conversions and Dalitz decays, and the cocktail method, which uses simulations of the background electron contributions based on the measurement of cross sections of the background electron sources [14]. The selection of electrons from beauty-hadron decays is based on the track impact parameter (d_0), defined as the distance of closest approach between the charged track and the interaction vertex in the transverse plane, that allows to statistically separate electrons from different sources. The contribution of electrons from beauty-hadron decays in Pb-Pb collisions is extracted from fits to the d_0 distributions of the measured electrons based on MC simulations of the distributions of each electron source. In pp collisions, the contribution of electrons from beauty-hadron decays is obtained with a requirement on the minimum d_0 and the contribution of the remaining electrons that do not originate from beauty-hadron

decays is obtained with the cocktail method.

The muon candidates are reconstructed with the muon spectrometer. The muon sample includes muons from heavy-flavour hadron decays and muons from background sources, which are mainly π and K decays. Background muons are estimated in pp collisions via MC simulations, while the estimation in p–Pb and Pb–Pb collisions is obtained using simulations of the decays of π and K, with the p_T distributions of these hadrons tuned to match the measurements at mid-rapidity and then extrapolated to the rapidity interval $2.5 < y < 4$ [15]. The forward-backward asymmetry of charged particles measured by the CMS Collaboration [16] is used to constrain the rapidity extrapolation in the analysis in p–Pb collisions. The contribution of muons from W decays, which is not negligible at high p_T, is subtracted statistically in the R_{AA} analysis using MC simulations.

3. Results

For all results presented here, the vertical error bars represent the statistical uncertainties, the horizontal error bars indicate the bin widths and the empty boxes represent the total systematic uncertainties. The boxes centered at unity in the nuclear modification factor figures represent the normalization uncertainty.
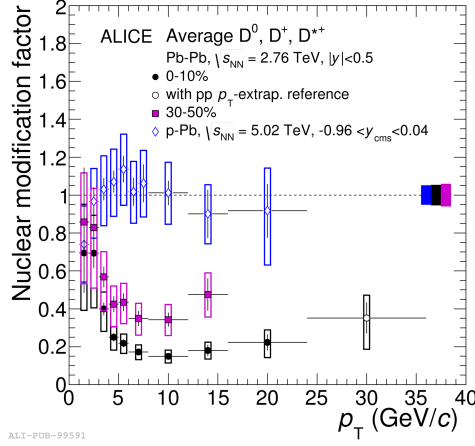
3.1 Nuclear modification factor

The nuclear modification factors in Pb–Pb collisions (R_{AA}) and in p–Pb collisions (R_{pPb}) are defined as:

$$R_{AA}(p_T) = \frac{1}{\langle T_{AA} \rangle} \frac{\mathrm{d}N_{AA}/\mathrm{d}p_T}{\mathrm{d}\sigma_{pp}/\mathrm{d}p_T}, \quad R_{pPb}(p_T) = \frac{1}{A} \frac{\mathrm{d}\sigma_{pPb}/\mathrm{d}p_T}{\mathrm{d}\sigma_{pp}/\mathrm{d}p_T}, \tag{3.1}$$

where $\mathrm{d}N_{AA}/\mathrm{d}p_T$ is the p_T-differential yield in Pb–Pb collisions, T_{AA} is the nuclear overlap function in Pb–Pb collisions, which is evaluated with the Glauber model [17], A is the mass number of the Pb nucleus, $\mathrm{d}\sigma_{pp}/\mathrm{d}p_T$ and $\mathrm{d}\sigma_{pPb}/\mathrm{d}p_T$ are the p_T-differential cross sections in pp and p–Pb collisions, respectively. Depending on the analysis, the pp references for the R_{AA} and R_{pPb} measurements are obtained by the measured cross sections in pp collisions at the same centre-of-mass energy or by a $\sqrt{s}$-scaling [18] of the measured cross sections in pp collisions at $\sqrt{s} = 2.76$ and/or 7 TeV. More details concerning the analyses can be found in [12, 19, 20].

Figure 1 shows the nuclear modification factor of prompt D mesons (average of D^0, D^+ and D^{*+}) as a function of p_T in minimum-bias p–Pb collisions at $\sqrt{s_{NN}} = 5.02$ TeV and in Pb–Pb collisions at $\sqrt{s_{NN}} = 2.76$ TeV in the 0–10% and 30–50% centrality classes [12]. No significant modification of the D-meson spectrum is observed in p–Pb collisions relative to pp collisions for $p_T > 2$ GeV/c, while a strong suppression of D mesons is observed in central and semi-central Pb–Pb collisions for $p_T > 3$ GeV/c. Therefore, the suppression observed in Pb–Pb collisions is predominantly due to final-state effects of the strongly-interacting matter created in those collisions.

Figure 2 shows the R_{AA} of D mesons (average of D^0, D^+ and D^{*+}) at mid-rapidity ($|y| < 0.5$) and in the interval $8 < p_T < 16$ GeV/c as a function of the average number of nucleons participating in the collision in each multiplicity class $\langle N_{part} \rangle$ [12], which represents the collision centrality. The result is compared with the R_{AA} of charged pions (left) at mid-rapidity ($|y| < 0.8$) and in the same p_T interval ($8 < p_T < 16$ GeV/c) [21] and with the R_{AA} of non-prompt J/ψ from B-meson decays (right) measured by the CMS Collaboration [22] in wider intervals of rapidity
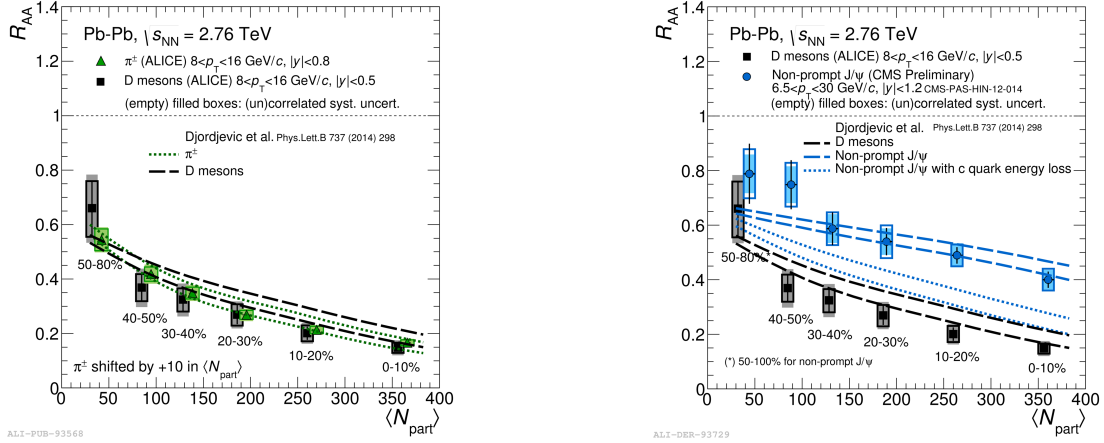
Figure 1: Nuclear modification factor of prompt D mesons (average of D^0, D^+ and D^{*+}) as a function of p_T in p–Pb collisions at $\sqrt{s_{NN}} = 5.02$ TeV and in Pb–Pb collisions at $\sqrt{s_{NN}} = 2.76$ TeV in the 0–10% and 30–50% centrality classes [12].
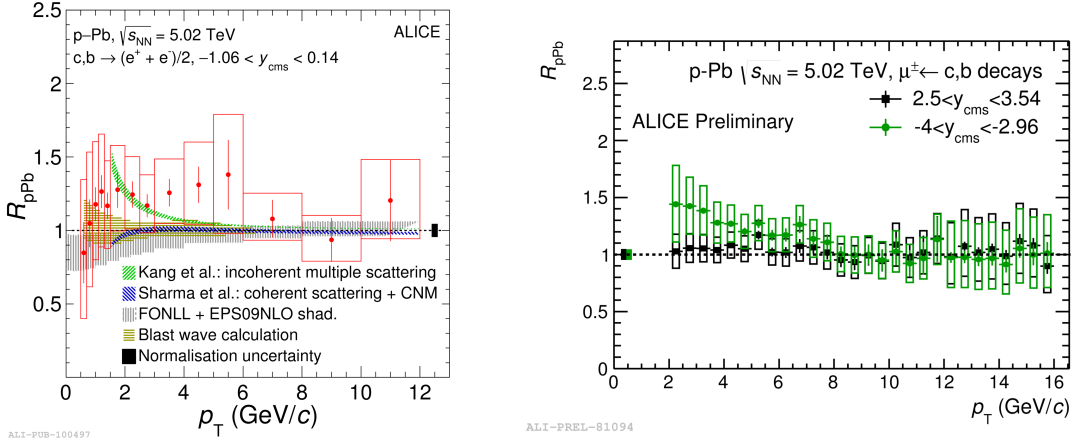
($|y| < 1.2$) and transverse momentum ($6.5 < p_T < 30$ GeV/c). The centrality dependence of the D-meson R_{AA} shows an increase of the suppression of D mesons towards central collisions (large $\langle N_{part} \rangle$ values), which is consistent with the qualitative expectation of the parton in-medium energy loss. The observed D-meson suppression is compatible, within uncertainties, with the observed suppression of charged pions in the same p_T interval, while it is found to be larger compared with the observed non-prompt J/ψ suppression. The comparison of R_{AA} of D mesons and non-prompt J/ψ from B-hadron decays hints at a difference in the suppression of particles originating from charm and beauty quarks in the most central collisions. The results are described by model calculations [23, 24] that include colour charge and mass dependence of the in-medium parton energy loss via radiative and collisional processes. The non-prompt J/ψ R_{AA} obtained using the charm-quark mass in the calculation of the energy loss of beauty quarks is used as a test for the origin of the difference in the R_{AA} of D mesons and non-prompt J/ψ. The corresponding result is closer to the D-meson R_{AA}, indicating that the observed difference in this model is predominantly due to the quark mass dependence of the parton energy loss.

Figure 3 shows the p_T dependence of the nuclear modification factor of electrons from heavy-flavour hadron decays in the interval $-1.06 < y_{cms} < 0.14$ [19] (left) and of muons from heavy-flavour hadron decays in the intervals $2.5 < y_{cms} < 3.54$ and $-4 < y_{cms} < -2.96$ (right) in p–Pb collisions at $\sqrt{s_{NN}} = 5.02$ TeV. The convention used for the rapidity sign in p–Pb collisions is negative for Pb-going direction, which addresses the orientation of the muon spectrometer, and positive for p-going one. No significant modification of the spectra of leptons from heavy-flavour hadron decays is observed in p–Pb collisions relative to pp collisions. The model calculations including only initial-state effects [13, 25, 26, 27, 28] describe the p_T dependence of the R_{pPb} of electrons from heavy-flavour hadron decays.

Figure 4 (left panel) shows the p_T dependence of the R_{AA} of electrons from heavy-flavour hadron decays at mid-rapidity ($|y| < 0.6$) and muons from heavy-flavour hadron decays at forward rapidity ($2.5 < y < 4$) in Pb–Pb collisions at $\sqrt{s_{NN}} = 2.76$ TeV in the 0–10% centrality class [20]. A strong suppression of electrons and muons from heavy-flavour hadron decays is observed for

Figure 2: D-meson R_{AA} at mid-rapidity ($|y| < 0.5$) in the interval $8 < p_T < 16$ GeV/c as a function of $\langle N_{part} \rangle$ and centrality class [12] compared with the $\pi^{\pm}$ R_{AA} at mid-rapidity ($|y| < 0.8$) in the interval $8 < p_T < 16$ GeV/c [21] (left) and with the non-prompt J/ψ R_{AA} measured by the CMS Collaboration in the intervals $|y| < 1.2$ and $6.5 < p_T < 30$ GeV/c [22] (right). The results are compared with model calculations [23, 24].
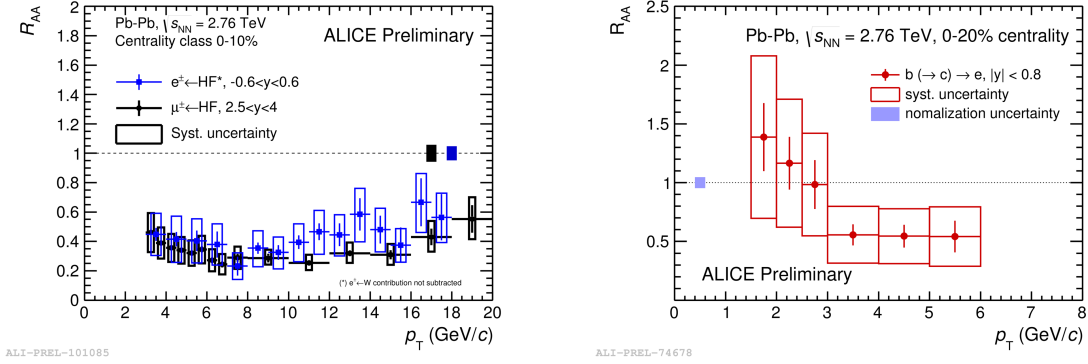

Figure 3: Left panel: R_{pPb} of electrons from heavy-flavour hadron decays as a function of p_T in the interval $-1.06 < y_{cms} < 0.14$ in minimum-bias p–Pb collisions at $\sqrt{s_{NN}} = 5.02$ TeV [19] compared with theoretical models [13, 25, 26, 27, 28]. Right panel: R_{pPb} of muons from heavy-flavour hadron decays as a function of p_T in the intervals $2.5 < y_{cms} < 3.54$ and $-4 < y_{cms} < -2.96$ in p–Pb collisions at $\sqrt{s_{NN}} = 5.02$ TeV.

$p_T > 3$ GeV/c. The observed suppression in central Pb–Pb collisions is predominantly due to the final-state effects of the created medium since the suppression cannot be explained by CNM effects, as shown in Figure 3. The p_T dependence of the R_{AA} of electrons from beauty-hadron decays at mid-rapidity ($|y| < 0.8$) in Pb–Pb collisions at $\sqrt{s_{NN}} = 2.76$ TeV in the 0–20% centrality class is shown in the right panel of Figure 4. The observed suppression of electrons from beauty-hadron decays for $p_T > 3$ GeV/c provides a hint for beauty quark in-medium energy loss.

3.2 Elliptic flow

The measurements of the elliptic flow of D mesons and electrons from heavy-flavour hadron decays presented here are performed with the event plane method, where the reaction plane angle

Figure 4: Left panel: R_{AA} of electrons from heavy-flavour hadron decays at mid-rapidity ($|y| < 0.6$) and muons from heavy-flavour hadron decays at forward rapidity ($2.5 < y < 4$) as a function of p_T in Pb–Pb collisions at $\sqrt{s_{NN}}$ = 2.76 TeV in the 0–10% centrality class. Right panel: R_{AA} of electrons from beauty-hadron decays at mid-rapidity ($|y| < 0.8$) as a function of p_T in Pb–Pb collisions at $\sqrt{s_{NN}}$ = 2.76 TeV in the 0–20% centrality class.
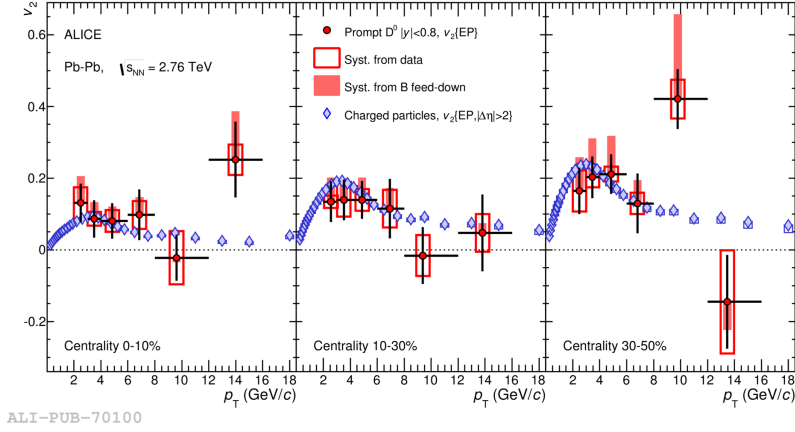
is estimated from the symmetry angle of the particle azimuthal distribution in the transverse plane. Depending on the analysis, the v_2 coefficient is obtained by:

$$v_2\{EP\} = \frac{1}{R_2}\langle\cos[2(\varphi - \Psi_2)]\rangle \text{ or } v_2\{EP\} = \frac{1}{R_2}\frac{\pi}{4}\frac{N_{in} - N_{out}}{N_{in} + N_{out}}, \quad (3.2)$$

where φ is the azimuthal angle of the heavy-flavour particles, Ψ_2 is the symmetry plane angle, R_2 is the event plane resolution correction, the angle brackets represent the average over the heavy-flavour particles in all events, and the factors N_{in} and N_{out} are the number of heavy-flavour particles along the in- and out-plane directions, respectively. The presented measurement of the elliptic flow of muons from heavy-flavour hadron decays is performed with the two-particle Q cumulants. In the case of the leptons from heavy-flavour hadron decays, the v_2 of the background leptons is estimated and the contribution is subtracted from the measured v_2 of inclusive leptons. More analysis details can be found in [15, 29, 30, 31].
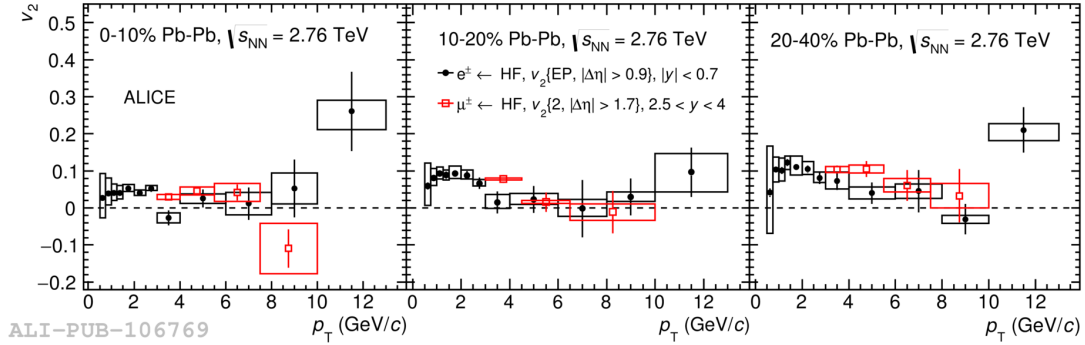
Figure 5 shows the v_2 of prompt D^0 mesons at mid-rapidity ($|y| < 0.8$) as a function of p_T in three centrality classes (0–10%, 10–30%, and 30–50%) in Pb–Pb collisions at $\sqrt{s_{NN}}$ = 2.76 TeV [29, 30]. A positive v_2 is observed with more than 5σ significance in the interval $2 < p_T < 6$ GeV/c in the 30–50% centrality class, which indicates a collective motion of low-p_T charm quarks in the medium. The centrality dependence of v_2 of prompt D^0 mesons hints for an increase of v_2 from central to peripheral collisions, which is consistent with the qualitative expectation of the evolution of the geometrical anisotropy of the overlap region of the colliding nuclei with the centrality. The prompt D^0-meson v_2 is compatible, within the uncertainties, with the charged-particle v_2 in the same centrality classes.

Figure 6 shows the v_2 of electrons from heavy-flavour hadron decays obtained with the event plane method at mid-rapidity ($|y| < 0.7$) and muons from heavy-flavour hadron decays obtained with the two-particle Q cumulant method at forward rapidity ($2.5 < y < 4$) [15] as a function of p_T in three centrality classes (0–10%, 10–20%, and 20–40%) in Pb–Pb collisions at $\sqrt{s_{NN}}$ = 2.76 TeV. A positive v_2 is observed with more than 3σ significance in the interval $1 < p_T^{e\leftarrow HF} < 3$ GeV/c for

Figure 5: v_2 of prompt D^0 mesons at mid-rapidity ($|y| < 0.8$) as a function of p_T in Pb–Pb collisions at $\sqrt{s_{NN}} = 2.76$ TeV in the 0–10% (left), 10–30% (central), and 30–50% (right) centrality classes [29, 30]. Results are compared with the charged-particle v_2 for the same centrality classes.

electrons from heavy-flavour decays and in the interval $3 < p_T^{\mu\leftarrow HF} < 5.5$ GeV/c for muons from heavy-flavour decays in the 20–40% centrality class, indicating that heavy quarks participate in the collective motion of the medium. Results also suggest an increasing of v_2 towards more peripheral collisions.
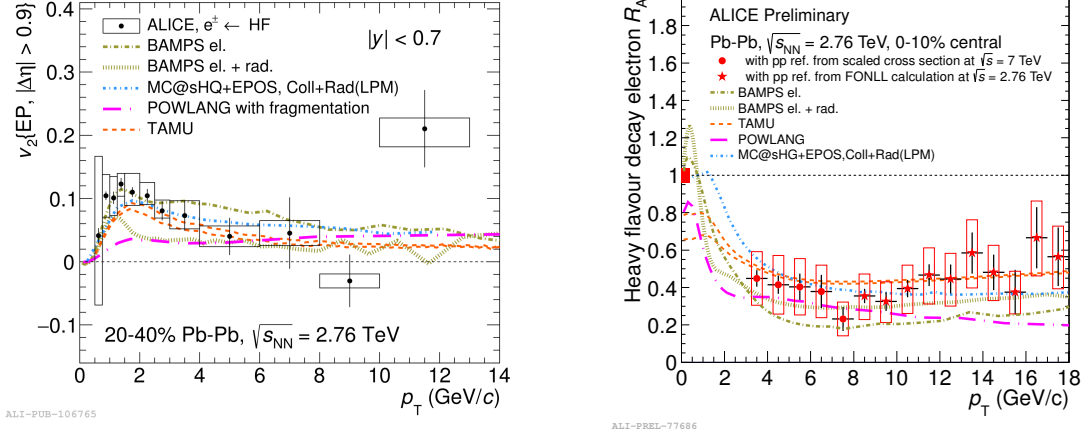

Figure 6: v_2 of electrons from heavy-flavour hadron decays at mid-rapidity ($|y| < 0.7$) [31] and muons from heavy-flavour hadron decays at forward rapidity ($2.5 < y < 4$) [15] as a function of p_T in Pb–Pb collisions at $\sqrt{s_{NN}} = 2.76$ TeV in the 0–10% (left), 10–20% (central) and 20–40% (right) centrality classes.

Figure 7 shows the comparison of v_2 (left) and R_{AA} (right) of electrons from heavy-flavour hadron decays as a function of p_T measured in Pb–Pb collisions in the 20–40% and 0–10% centrality classes, respectively, with model calculations [32, 33, 34, 35]. The models including interactions of the heavy quarks with the medium constituents can describe qualitatively the v_2 of electrons from heavy-flavour hadron decays. The simultaneous comparison of R_{AA} and v_2 measurements to model calculations provides constraints for the models.

3.3 Azimuthal angular correlations

The azimuthal angular correlation between heavy-flavour particles (trigger) and charged par-

Figure 7: Left panel: v_2 of electrons from heavy-flavour hadron decays at mid rapidity ($|y| < 0.7$) as a function of p_T measured in Pb–Pb collisions at $\sqrt{s_{NN}} = 2.76$ TeV in the 20–40% centrality class [31]. Right panel: R_{AA} of electrons from heavy-flavour hadron decays at mid rapidity ($|y| < 0.6$) as a function of p_T measured in Pb–Pb collisions at $\sqrt{s_{NN}} = 2.76$ TeV in the 0–10% centrality class. For both panels, results are compared with parton transport models [32, 33, 34, 35].
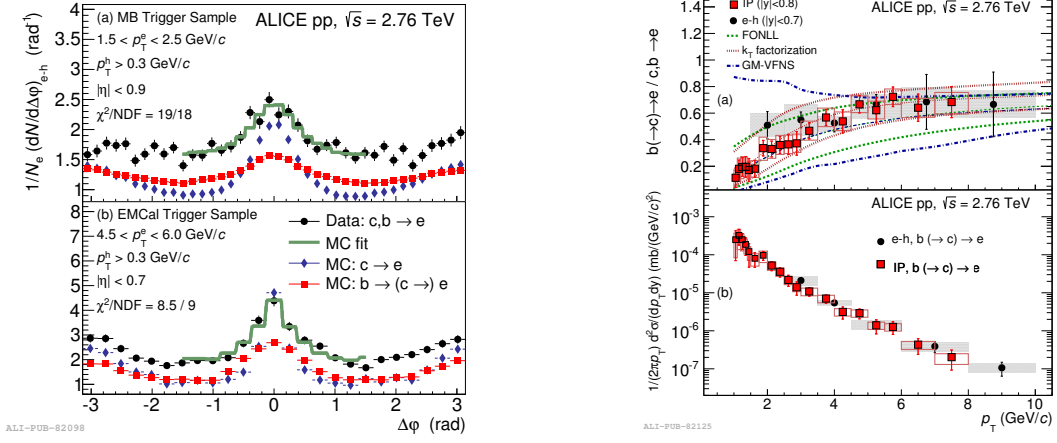
ticles (associated) is defined as the differential yield of trigger-associated particle pairs in azimuth ($\Delta\varphi$) and in pseudorapidity ($\Delta\eta$):

$$C(\Delta\varphi, \Delta\eta) = \frac{1}{N_{trigger}} \frac{d^2 N_{pair}}{d\Delta\varphi d\Delta\eta}, \tag{3.3}$$

where $N_{trigger}$ is the number of trigger particles and N_{pair} is the number of trigger-associated particle pairs. The correlation distributions are corrected for the limited acceptance and spatial inhomogeneities of the detector using the event mixing technique and for the efficiency of the trigger and associated particle reconstructions. Details of the analyses can be found in [36, 37].
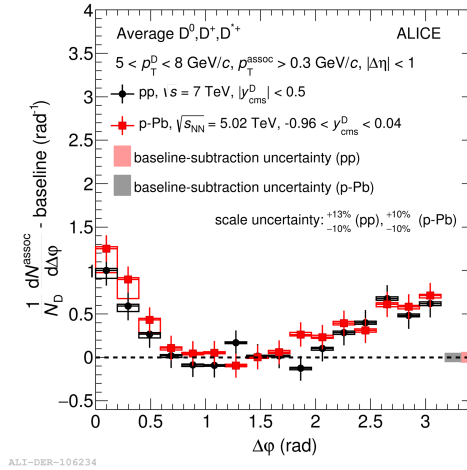
Figure 8 (left panel) shows the azimuthal angular correlation between electrons from heavy-flavour hadron decays in two intervals of pseudorapidity ($|\eta| < 0.9$ and $|\eta| < 0.7$) and transverse momentum ($1.5 < p_T < 2.5$ GeV/c and $4.5 < p_T < 6$ GeV/c) and charged hadrons for $p_T > 0.3$ GeV/c in pp collisions at $\sqrt{s} = 2.76$ TeV [36]. The near ($\Delta\varphi \approx 0$) and away side ($\Delta\varphi \approx \pi$) peaks are clearly visible. The relative contribution of electrons from beauty-hadron decays to the yield of electrons from heavy-flavour decays (r_b) is obtained with a fit to the measured correlation distributions using a MC simulation with PYTHIA [38] of the correlation distributions of electrons from beauty and charm hadron decays, as shown in the left panel of Figure 8. The width of the near-side peak is larger for electrons from beauty-hadron decays than from charm-hadron decays due to the different mass and decay kinematics of charm and beauty hadrons. The factor r_b is shown in the top right panel of Figure 8 and compared with the result obtained using the impact parameter method and predictions from different pQCD calculations [13, 39, 40]. The contribution of electrons from beauty-hadron decays to the yield of electrons from heavy-flavour decays increases with p_T and reaches 50% at approximately 4 GeV/c. The r_b parameter is used to scale the measured heavy-flavour decay electron cross section in pp collisions at $\sqrt{s} = 2.76$ TeV [41] in order to obtain the cross section of electrons from beauty hadron decays. The corresponding result (bottom right panel

of Figure 8) shows a good agreement with the one obtained using the impact parameter method.

Figure 8: Left panel: azimuthal angular correlation between electrons from heavy-flavour hadron decays in two intervals of pseudorapidity ($|\eta| < 0.9$ and $|\eta| < 0.7$) and transverse momentum ($1.5 < p_T < 2.5$ GeV/c and $4.5 < p_T < 6$ GeV/c) and charged hadrons for $p_T > 0.3$ GeV/c in pp collisions at $\sqrt{s} = 2.76$ TeV. Right panel: (a) relative contribution of electrons from beauty-hadron decays to the heavy-flavour decay electron yield (r_b) compared with the result obtained using the impact parameter method and different pQCD calculations [13, 39, 40]. (b) p_T-differential inclusive production cross section of electrons from beauty-hadron decays compared with the result obtained using the impact parameter method.

Figure 9 shows the azimuthal correlation of D mesons in the p_T interval $5 < p_T < 8$ GeV/c and charged particles with $p_T > 0.3$ GeV/c in p–Pb collisions at $\sqrt{s_{NN}} = 5.02$ TeV and in pp collisions at $\sqrt{s} = 7$ TeV. The correlation pattern in pp collisions is compatible with the one measured in p–Pb collisions after the baseline subtraction. Therefore, no modification of the azimuthal correlation of D mesons and charged particles in p–Pb collisions is observed with the current uncertainties.

Figure 9: Comparison of the azimuthal angular correlation, after the baseline subtraction, of D mesons in the interval $5 < p_T < 8$ GeV/c and charged particles for $p_T > 0.3$ GeV/c in p–Pb collisions at $\sqrt{s_{NN}} = 5.02$ TeV and in pp collisions at $\sqrt{s} = 7$ TeV [37].

4. Conclusions

We presented the ALICE results on the nuclear modification factor, elliptic flow, and azimuthal angular correlations of D mesons and electrons from heavy-flavour decays at mid-rapidity and muons from heavy-flavour decays at forward rapidity.

No significant modification of the spectra of D mesons and of electrons and muons from heavy-flavour hadron decays is observed in p–Pb collisions relative to pp collisions, while results in central and semi-central Pb–Pb collisions reveal a strong suppression for $p_T > 3$ GeV/c. Therefore, no significant CNM effect on the heavy-flavour particle production is found and the suppression observed in Pb–Pb collisions is predominantly due to the strong final-state effects of the created medium. The comparison of the R_{AA} of D mesons and non-prompt J/ψ from B-hadron decays indicates a difference in the suppression of particles originating from charm and beauty quarks in the most central collisions. The measurement of the R_{AA} of electrons from beauty-hadron decays in the 20% most central Pb–Pb collisions shows a suppression for $p_T > 3$ GeV/c, which provides a hint for the in-medium energy loss of beauty quarks.

A positive v_2 of prompt D^0 mesons is observed with more than 5σ significance in the interval $2 < p_T < 6$ GeV/c in the 30–50% centrality class, which indicates a collective motion of low-p_T charm quarks in the medium. The measured v_2 of electrons and muons from heavy-flavour hadron decays is positive with more than 3σ significance in the intervals $1 < p_T^{e\leftarrow HF} < 3$ GeV/c and $3 < p_T^{\mu\leftarrow HF} < 5.5$ GeV/c in Pb–Pb collisions at $\sqrt{s_{NN}}$ = 2.76 TeV in the 20–40% centrality class, indicating that heavy quarks participate in the collective motion of the medium. The centrality dependence of v_2 of the measured heavy-flavour particles hints for an increase from central to peripheral collisions, which is consistent with the qualitative expectation of the evolution of the geometrical anisotropy of the overlap region of the colliding nuclei with the centrality.

The azimuthal angular correlations between electrons from heavy-flavour hadron decays and charged particles provide the relative contribution of electrons from beauty-hadron decays to the yield of electrons from heavy-flavour decays. The obtained relative contribution in pp collisions at $\sqrt{s}$ = 2.76 TeV increases with p_T and reaches 50% at approximately 4 GeV/c. No modification of the azimuthal angular correlation between D mesons and charged particles in p–Pb collisions at $\sqrt{s_{NN}}$ = 5.02 TeV is observed, with the current uncertainties, with respect to the measured one in pp collisions at $\sqrt{s}$ = 7 TeV.

References

[1] F. Karsch, J. Phys. Conf. Ser. 46 (2006) 122–131.

[2] P. Petreczky, arXiv:1301.6188 [hep-lat] (2013).

[3] Yu. L. Dokshitzer and D. E. Kharzeev, Phys. Lett. B 519 (2001) 199–206.

[4] N. Armesto, C. Salgado, and U. Wiedemann, Phys. Rev. D 69 (2004) 114003.

[5] S. Wicks, W. Horowitz, M. Djordjevic, and M. Gyulassy, Nucl. Phys. A 783 (2007) 493–496.

[6] K. Eskola, H. Paukkunen, and C. Salgado, J. High Energy Phys. 04 (2009) 065.

[7] D. de Florian and R. Sassot, Phys. Rev. D 69 (2004) 074028.

[8] H. Fujii and K. Watanabe, Nucl. Phys. A 915 (2013) 1.

[9] CMS Collaboration, Phys. Lett. B 718 (2013) 795–814.

[10] ALICE Collaboration, J. Inst. 3 (2008) S08002.

[11] ALICE Collaboration, Int. J. Mod. Phys. A 29 (2014) 1430044.

[12] ALICE Collaboration, J. High Energy Phys. 03 (2016) 81.

[13] M. Cacciari, M. Greco, and P. Nason, J. High Energy Phys. 9805 (1998) 7 ; M. Cacciari, S. Frixione and P. Nason, J. High Energy Phys. 0103 (2001) 6.

[14] ALICE Collaboration, Phys. Rev. D 86 (2012) 112007.

[15] ALICE Collaboration, Phys. Lett. B 753 (2016) 41–56.

[16] CMS Collaboration, CMS-PAS-HIN-12-017.

[17] M. L. Miller, K. Reygers, S. J. Sanders, and P. Steinberg, Ann. Rev. Nucl. Part. Sci. 57, 205 (2007).

[18] R. Averbeck, N. Bastid, Z. Conesa del Valle, P. Crochet, and A. Dainese, X. Zhang, arXiv:1107.3243 [hep-ph] (2011).

[19] ALICE Collaboration, Phys. Lett. B 754 (2016) 81–93.

[20] ALICE Collaboration, Phys. Rev. Lett. 109 (2012) 112301.

[21] ALICE Collaboration, Phys. Lett. B 736 (2014) 196–207.

[22] CMS Collaboration, J. High Energy Phys. 1205 (2012) 063.

[23] M. Djordjevic, M. Djordjevic, and B. Blagojevic, Ó Phys. Lett. B 737 (2014) 298Ð302.

[24] A. Andronic, F. Arleo, R. Arnaldi, A. Beraudo, E. Bruna, et al., arXiv:1506.03981 [nucl-ex] (2015).

[25] Z.-B. Kang, I. Vitev, E. Wang, H. Xing, and C. Zhang, Phys. Lett. B 740 (2015) 23–29.

[26] R. Sharma, I. Vitev, and B.-W. Zhang, Phys. Rev. C 80 (2009) 054902.

[27] A.M. Sickles, Phys. Lett. B 731 (2014) 51Ð56.

[28] K.J. Eskola, H. Paukkunen, and C.A. Salgado, J. High Energy Phys. 04 (2009) 065.

[29] ALICE Collaboration, Phys. Rev. Lett. 111 (2013) 102301.

[30] ALICE Collaboration, Phys. Rev. C 90 (2014) 034904.

[31] ALICE Collaboration, arXiv:1606.00321 [nucl-ex] (2016).

[32] J. Uphoff, O. Fochler, Z. Xu, and C. Greiner, Phys. Lett. B 717 (2012) 430–435.

[33] M. He, R. J. Fries, and R. Rapp, arXiv:1208.0256 [nucl-th] (2012).

[34] M. Monteno, W. M. Alberico, A. Beraudo, A. De Pace, A. Molinari, M. Nardi, and F. Prino, J. Phys. G. 38 (2011) 124144.

[35] P. B. Gossiaux, R. Bierkandt, and J. Aichelin, Phys. Rev. C 79 (2009) 044906.

[36] ALICE Collaboration, arXiv:1405.4144 [nucl-ex] (2014).

[37] ALICE Collaboration, arXiv:1605.06963 [nucl-ex] (2016).

[38] T. Sjostrand, S. Mrenna, and P. Z. Skands, J. High Energy Phys. 05 (2006) 26.

[39] P. Bolzoni and G. Kramer, Nucl. Phys. B 872 (2013) 253.

[40] R. Maciula and A. Szczurek, Phys. Rev. D 87 9 (2013) 094022.

[41] ALICE Collaboration, arXiv:1405.4117 [nucl-ex] (2014).